Available online at www.sciencedirect.com
SCIENCE DIRECT
Journal of Magnetism and Magnetic Materials 305 (2006) 141–146
Journal of magnetism and magnetic materials
www.elsevier.com/locate/jmmm

Quantum theory of tunneling magnetoresistance in GaMnAs/GaAs/GaMnAs heterostructures

Alireza Saffarzadeh[a,*], Ali A. Shokri[a,b]

[a]Department of Physics, Tehran Payame-Noor University, Fallahpour St. Nejatollahi St. Tehran, Iran
[b]Computational Physical Sciences Research Laboratory, Department of Nano-Science, Institute for studies in theoretical Physics and Mathematics (IPM), P.O. Box 19395-5531, Tehran, Iran

Received 20 August 2005; received in revised form 29 November 2005
Available online 28 December 2005

Abstract

Using a quantum theory including spin-splitting effect in diluted magnetic semiconductors, we study the dependence of tunneling magnetoresistance (TMR) on barrier thickness, temperature and applied voltage in GaMnAs/GaAs/GaMnAs heterostructures. TMR ratios more than 65% are obtained at zero temperature, when one GaAs monolayer (≈ 0.565 nm) is used as a tunnel barrier. It is also shown that the TMR ratio decreases rapidly with increasing barrier thickness and applied voltage; however, at high voltages and low thicknesses, the TMR first increases and then decreases. Our model calculations well explain the main features of the recent experimental observations.

PACS: 72.25.−b; 73.23.−b; 75.50.Pp; 85.75.−d

Keywords: Diluted magnetic semiconductor; Tunnel magnetoresistance; Spin-polarized transport

1. Introduction

In the past few years, tunneling magnetoresistance (TMR) in magnetic tunnel junctions (MTJs) has attracted much attention due to the possibility of its application in magnetic memories, magnetic field sensors and quantum computing devices [1,2]. In a common MTJ, the TMR between two ferromagnetic electrodes separated by an insulator layer depends on the spin polarization of the ferromagnetic electrodes and spin-dependent tunneling rates [3–5]. For such structures, much efforts have been made to increase the TMR ratio, which can be defined by the relative change in the current densities. Recently, a large TMR ratio as much as 60% has been reported in Co–Fe/Al–O/Co–Fe junctions [6] which opened a new era of technical applications of the tunnel junctions.

Using ferromagnetic semiconductors (FMSs), such as EuS, the TMR has also been investigated in single [7–10] and double [11–14] magnetic barrier junctions. In these structures, the FMSs which act as spin filters are used as tunnel barriers. Therefore, the MTJs using these materials are able to produce highly spin-polarized current and high values for TMR. However, the Curie temperature in most of FMSs is much lower than room temperature [15].

On the other hand, coexistence of ferromagnetism and semiconducting properties in diluted magnetic semiconductors (DMSs) has opened the prospect of developing devices which make it possible to combine the information processing and data storage in the same material [16,17]. In the magnetic semiconductors, the exchange interaction between the itinerant carriers in the semiconducting band and the localized spins on magnetic impurity ions leads to spectacular magneto-optical effects, such as giant Faraday rotation or Zeeman splitting. Among different types of DMSs, $Ga_{1-x}Mn_xAs$ is one of the most suitable materials for use in spintronic devices. In this kind of materials, a

*Corresponding author. Tel.: +98218800252; fax: +98218808203.
E-mail addresses: a-saffar@tehran.pnu.ac.ir (A. Saffarzadeh), aashokri@nano.ipm.ac.ir (A.A. Shokri).

0304-8853/$ - see front matter © 2005 Elsevier B.V. All rights reserved.
doi:10.1016/j.jmmm.2005.12.001

fraction of the group-III sublattice is replaced at random by Mn ions which act as acceptors. According to the strong Hund coupling, the five 3d electrons in a Mn^{2+} ion give rise to a localized magnetic moment. The DMSs based on III–V semiconductors, like $Ga_{1-x}Mn_xAs$ compounds, exhibit ferromagnetism with Curie temperature as high as 110 K for Mn doping of around $x = 0.05$. The origin of ferromagnetism in the GaAs-based DMSs can be demonstrated through the p–d exchange coupling between the itinerant holes in the valence band of GaAs and the spin of magnetic impurities [16–18]. In spite of low Curie temperature of $Ga_{1-x}Mn_xAs$, the use of $Ga_{1-x}Mn_xAs$-based III–V heterostructures as MTJs presents several advantages. The possible advantages include not only simple integration with existing semiconductor technology, but also relatively straightforward fabrication of high-quality epitaxial structures, easily controlled physical and electronic structure, and the integration of quantum heterostructures which is easier than in any other materials system [19].

The spontaneous magnetization and the feasibility of preparing GaAs-based DMS [20] are stimulated much attention for studying the spin-polarized transport phenomena in $Ga_{1-x}Mn_xAs$/(GaAs or AlAs) heterostructures. Recently, Chiba et al. [21] observed a TMR ratio of 5.5% at 20 K in a GaMnAs tunnel junction. Also, Tanaka and Higo [22] reported TMR ratios more than 70% at 8 K in GaMnAs/AlAs/GaMnAs heterostructures. Moreover, recent analyses of temperature dependence of current–voltage characteristics of GaMnAs/GaAs/p-GaAs p-i-p diodes have shown that GaAs intermediary layer which is a nonmagnetic semiconductor (NMS), acts as a barrier (87–140 meV) for holes injected from GaMnAs [23]. In this regard, a large TMR ratio of 290% has been observed at 0.39 K in GaMnAs/GaAs/GaMnAs heterostructures, around zero applied bias [24]. Such a high TMR ratio is a result of high spin polarization of DMS electrodes and the high quality of sample and interfaces between GaMnAs and GaAs layer. Interlayer exchange interaction is another effect which has also been studied in $Ga_{0.96}Mn_{0.04}As$/GaAs superlattices, where an oscillatory behavior with varying thickness of GaAs spacer is predicted [25].

From a theoretical point of view, the TMR has also been investigated in GaMnAs/AlAs/GaMnAs heterostructures. Tanaka and Higo [22] calculated the dependence of TMR on AlAs thickness using the tight-binding theory including that the parallel wave vector of carriers is conserved in tunneling process. The results showed that the TMR ratio decreases rapidly with increasing barrier thickness. Also, Tao et al. [26] studied the AlAs thickness dependence of TMR using the transfer matrix approach. Their treatment, however, is somewhat questionable, because they did not apply the boundary conditions for derivatives of wave functions correctly. When the materials are different, it is the normal mass flux that must be continuous.

In the present work, we study theoretically the spin-polarized transport in GaMnAs/GaAs/GaMnAs tunnel junctions by considering the effect of spontaneous magnetization of GaMnAs layers. The temperature dependence of the spin-splitting energy is calculated for DMSs within the mean-field approximation. Using the transfer matrix method and the nearly-free-carrier approximation we will study the TMR and spin polarization of tunneling carriers in terms of the barrier thickness and bias voltage at all temperatures. We assume that the carrier wave vector parallel to the interfaces and the carrier spin are conserved in the tunneling process through the whole system.

The paper is organized as follows. In Section 2, the model is described and then the spin polarization and the TMR for DMS/NMS/DMS structures are formulated. Next, the temperature dependence of spin-splitting energy is obtained for DMS, within the mean-field framework. In Section 3, numerical results obtained for a typical tunnel junction are discussed. The results of this work are summarized in Section 4.

2. Description of model and formalism

In order to investigate the spin-dependent transport properties in MTJs based on DMS materials, we consider two semi-infinite DMS electrodes separated by a NMS layer, which acts as a barrier, in the presence of DC applied bias V_a. For simplicity, we assume that the two DMS electrodes are made of the same materials and all of the interfaces are flat. In the framework of the parabolic-band effective mass approximation, the longitudinal part of the one-hole Hamiltonian can be written as

$$H_x = -\frac{\hbar^2}{2m_j^*}\frac{d^2}{dx^2} + U_j(x) - \mathbf{h}_j^{MF}\cdot\sigma, \tag{1}$$

where m_j^* ($j = 1-3$) is the hole effective mass in the jth layer, and

$$U_j(x) = \begin{cases} 0, & x<0, \\ E_F + \phi - eV_a x/d, & 0<x<d, \\ -eV_a, & x>d, \end{cases} \tag{2}$$

where d is the barrier thickness, E_F is the Fermi energy in the left electrode, measured from the middle point between the edges of the two spin subbands, and ϕ is the barrier height measured from the Fermi level. $-\mathbf{h}_j^{MF}\cdot\sigma$ is the internal exchange energy where $\mathbf{h}_j^{MF}$ is the molecular field in the jth DMS electrode and σ is the conventional Pauli spin operator.

The Schrödinger equation for a biased barrier layer can be simplified by a coordinate transformation whose solution is the linear combination of the Airy function $Ai[\rho(x)]$ and its complement $Bi[\rho(x)]$ [27]. Considering all three regions of the DMS/NMS/DMS junction, the eigenfunctions of the Hamiltonian (1) with eigenvalue E_x

have the following forms:

$$\psi_{j,\sigma}(x)=\begin{cases} A_{1\sigma}e^{ik_{1\sigma}x}+B_{1\sigma}e^{-ik_{1\sigma}x}, & x<0,\\ A_{2\sigma}\mathrm{Ai}[\rho(x)]+B_{2\sigma}\mathrm{Bi}[\rho(x)], & 0<x<d,\\ A_{3\sigma}e^{ik_{3\sigma}x}+B_{3\sigma}e^{-ik_{3\sigma}x}, & x>d, \end{cases} \tag{3}$$

where

$$k_{1\sigma}=\sqrt{2m_1^*(E_x+h_0\sigma)}/\hbar, \tag{4}$$

$$k_{3\sigma}^{(\Gamma)}=\sqrt{2m_3^*(E_x+eV_a+\Gamma h_0\sigma)}/\hbar \tag{5}$$

are the hole wave vectors along the x-axis. Here, σ are the hole spin components ±1 (or $\uparrow,\downarrow$), $h_0=|\mathbf{h}_j^{\mathrm{MF}}|$ and $\Gamma=+1(-1)$ for parallel (antiparallel) alignment of the magnetizations. The coefficients $A_{j\sigma}$ and $B_{j\sigma}$ are constants to be determined from the boundary conditions, while

$$\rho(x)=-\frac{d}{eV_a\lambda}\left(E_F+\phi-E_x-\frac{x}{d}eV_a\right), \tag{6}$$

with

$$\lambda=\left[\frac{-\hbar^2 d}{2m_2^* eV_a}\right]^{1/3}. \tag{7}$$

Although the transverse momentum $\mathbf{k}_\parallel$ is omitted from the above notations, the summation over $\mathbf{k}_\parallel$ is carried out in our calculations.

Upon applying the boundary conditions such that the wave functions and their first derivatives are matched at each interface point x_j, i.e. $\psi_{j,\sigma}(x_j)=\psi_{j+1,\sigma}(x_j)$ and $(m_j^*)^{-1}[\mathrm{d}\psi_{j,\sigma}(x_j)/\mathrm{d}x]=(m_{j+1}^*)^{-1}[\mathrm{d}\psi_{j+1,\sigma}(x_j)/\mathrm{d}x]$, we obtain a matrix formula that connects the coefficients $A_{1\sigma}$ and $B_{1\sigma}$ with the coefficients $A_{3\sigma}$ and $B_{3\sigma}$ [8]. Since there is no reflection in region 3, the coefficient $B_{3\sigma}$ in Eq. (3) is zero and the transmission coefficient of the spin σ hole, which is defined as the ratio of the transmitted flux to the incident flux can be written as follows:

$$T_\sigma^{(\Gamma)}(E_x,V_a)=\frac{4m_1^*m_3^*k_{1\sigma}k_{3\sigma}^{(\Gamma)}}{(\pi\lambda m_2^*)^2}[(\alpha k_{1\sigma}k_{3\sigma}^{(\Gamma)}+\delta m_1^*m_3^*)^2+(\beta m_3^*k_{1\sigma}-\gamma m_1^*k_{3\sigma}^{(\Gamma)})^2]^{-1}, \tag{8}$$

where the following abbreviations are used

$$\alpha=\mathrm{Ai}[\rho(0)]\mathrm{Bi}[\rho(d)]-\mathrm{Bi}[\rho(0)]\mathrm{Ai}[\rho(d)], \tag{9}$$

$$\beta=\frac{1}{\lambda m_2^*}\{\mathrm{Ai}[\rho(0)]\mathrm{Bi}'[\rho(d)]-\mathrm{Bi}[\rho(0)]\mathrm{Ai}'[\rho(d)]\}, \tag{10}$$

$$\gamma=\frac{1}{\lambda m_2^*}\{\mathrm{Ai}'[\rho(0)]\mathrm{Bi}[\rho(d)]-\mathrm{Bi}'[\rho(0)]\mathrm{Ai}[\rho(d)]\}, \tag{11}$$

$$\delta=\frac{1}{(\lambda m_2^*)^2}\{\mathrm{Ai}'[\rho(0)]\mathrm{Bi}'[\rho(d)]-\mathrm{Bi}'[\rho(0)]\mathrm{Ai}'[\rho(d)]\}. \tag{12}$$

Here, $\mathrm{Ai}'[\rho(x)]$ and $\mathrm{Bi}'[\rho(x)]$ are the first derivatives of the Airy functions.

2.1. Current densities and TMR

The spin-dependent current density for a MTJ with a given applied bias V_a and at temperature T can be calculated within the nearly-free-hole approximation [28]:

$$J_\sigma^{(\Gamma)}(V_a)=\frac{em_1^*k_BT}{4\pi^2\hbar^3}\int_{E_0^\sigma}^{\infty}T_\sigma^{(\Gamma)}(E_x,V_a)\ln\times\left\{\frac{1+\exp[(E_F-E_x)/k_BT]}{1+\exp[(E_F-E_x-eV_a)/k_BT]}\right\}\mathrm{d}E_x, \tag{13}$$

and, at $T=0$ K,

$$J_\sigma^{(\Gamma)}(V_a)=\frac{em_1^*}{4\pi^2\hbar^3}\left[eV_a\int_{E_0^\sigma}^{E_F-eV_a}T_\sigma^{(\Gamma)}(E_x,V_a)\,\mathrm{d}E_x+\int_{E_F-eV_a}^{E_F}(E_F-E_x)T_\sigma^{(\Gamma)}(E_x,V_a)\,\mathrm{d}E_x\right], \tag{14}$$

where k_B is the Boltzmann constant and E_0^σ is the lowest possible energy that will allow transmission and is given by $E_0^\uparrow=\max\{-h_0,-eV_a-\Gamma h_0\}$ for spin-up holes and $E_0^\downarrow=h_0$ for spin-down ones. It is clear that the tunnel current is modulated by the magnetic configurations of the both DMS electrodes.

The degree of spin polarization for the tunnel current is defined by $P=(J_\uparrow-J_\downarrow)/(J_\uparrow+J_\downarrow)$, where $J_\uparrow$ ($J_\downarrow$) is the spin-up (spin-down) current density. For the present structure, we obtain this quantity when the magnetizations of two DMS electrodes are in parallel alignment. For studying the TMR, the spin currents in the both parallel and antiparallel alignments are calculated. In this case, the TMR can be defined as

$$\mathrm{TMR}=\frac{(J_\uparrow^{\mathrm{p}}+J_\downarrow^{\mathrm{p}})-(J_\uparrow^{\mathrm{ap}}+J_\downarrow^{\mathrm{ap}})}{J_\uparrow^{\mathrm{ap}}+J_\downarrow^{\mathrm{ap}}}, \tag{15}$$

where $J_{\uparrow,\downarrow}^{\mathrm{p(ap)}}$ corresponds to the current density in the parallel (antiparallel) alignment of the magnetizations in the FM electrodes, for a spin-up ($\uparrow$) or spin-down ($\downarrow$) hole.

2.2. Temperature dependence of spin-splitting energy

In the following, we develop the formalism for calculating of temperature dependence of the spin-splitting energy in the DMS electrodes using the mean-field theory. At the first step, we consider the magnetic Hamiltonian for one itinerant hole with spin $\mathbf{s}$ located at $\mathbf{r}$ and one Mn ion with spin $\mathbf{S}$ located at $\mathbf{R}$. Both of these magnetic subsystems can be described as [29]

$$H^{\mathrm{h}}=J_{\mathrm{pd}}\sum_I\mathbf{s}\cdot\mathbf{S}_I\,\delta(\mathbf{r}-\mathbf{R}_I) \tag{16}$$

and

$$H^{\mathrm{Mn}}=J_{\mathrm{pd}}\sum_i\mathbf{s}_i\cdot\mathbf{S}\,\delta(\mathbf{r}_i-\mathbf{R}). \tag{17}$$

Here, J_{pd} is the hole–Mn exchange coupling constant, μ_B is the Bohr magneton, g_h and g_{Mn} are the Landé g-factor for holes and Mn ions, respectively. In the mean-field

approximation, $H^{h} \longrightarrow H^{h}_{MF} \equiv g_{h}\mu_{B}\mathbf{s}\cdot\mathbf{h}^{h}$ and $H^{Mn} \longrightarrow H^{Mn}_{MF} \equiv g_{Mn}\mu_{B}\mathbf{S}\cdot\mathbf{h}^{Mn}$, where $\mathbf{h}^{h}$ and $\mathbf{h}^{Mn}$ are respectively the effective magnetic fields acting upon holes and magnetic impurities, and can be given as

$$h^{h} = \frac{1}{g_{h}\mu_{B}} J_{pd} N_{Mn} \langle S_z \rangle \tag{18}$$

and

$$h^{Mn} = \frac{1}{g_{Mn}\mu_{B}} J_{pd} M^{h}. \tag{19}$$

Here, $N_{Mn} = 4x/a_0^3$ is the density of Mn ions, with a_0^3 being the unit cell volume. $\mathbf{M}^{h} = \sum_i \langle \mathbf{s}_i \rangle \delta(\mathbf{r}_i - \mathbf{R})$ is the magnetization density of the hole subsystem, which is assumed to be uniform within the length scale of the magnetic interactions, so the magnetic response of the Fermi sea holes to the effective field h^{h}, is given by

$$M^{h} = g_{h}\mu_{B} s^2 D^{h}(E_F) h^{h}, \tag{20}$$

where the density of states of the hole gas with effective mass m^* and the hole concentration p is $D^{h}(E_F) = (3\pi^2)^{-2/3}(3m^*/\hbar^2)p^{1/3}$. On the other hand, the magnetic response of the impurity spin to the effective field h^{Mn} is given by

$$M^{Mn} = g_{Mn}\mu_{B} N_{Mn} \langle S_z \rangle = g_{Mn}\mu_{B} N_{Mn} S \mathscr{B}_S\left(\frac{g_{Mn}\mu_{B} S h^{Mn}}{k_{B}T}\right), \tag{21}$$

where

$$\mathscr{B}_S(x) = \left(\frac{2S+1}{2S}\right)\coth\left(\frac{2S+1}{2S}x\right) - \left(\frac{1}{2S}\right)\coth\left(\frac{1}{2S}x\right) \tag{22}$$

is the Brillouin function. Therefore, within the spirit of a mean-field framework the magnetization of Mn subsystem is then given by

$$M^{Mn} = g_{Mn}\mu_{B} N_{Mn} S \mathscr{B}_S\left(\frac{J_{pd} S}{2k_{B}T} M^{h}\right), \tag{23}$$

which should be determined self-consistently with the hole magnetization

$$M^{h} = \frac{J_{pd} D^{h}(E_F)}{2 g_{Mn}\mu_{B}} M^{Mn}. \tag{24}$$

Also, the ferromagnetic transition temperature T_C can be obtained using the expansion for the Brillouin function $\mathscr{B}_S(x)$, when $x \ll 1$. In this regard, T_C is found as

$$T_C = (J_{pd} s)^2 N_{Mn} \frac{S(S+1) D(E_F)}{3k_{B}}. \tag{25}$$

Now, the temperature dependence of spin-splitting energy in the jth DMS electrode can be obtained as $\Delta_j = 2|\mathbf{h}_j^{MF}|$, where the molecular field is $\mathbf{h}_j^{MF} = (J_{pd}/2g_{Mn}\mu_{B})\mathbf{M}_j^{Mn}$.

3. Numerical results and discussions

Numerical calculations have been carried out to investigate the effects of barrier thickness, temperature and applied voltage on spin-dependent transport in a typical $Ga_{1-x}Mn_xAs/GaAs/Ga_{1-x}Mn_xAs$ tunnel structure. We have chosen $Ga_{1-x}Mn_xAs$ and GaAs because of the same crystal structures and lattice constants [22]. The relevant parameters for $Ga_{1-x}Mn_xAs$ electrodes are chosen as $a_0 = 5.65\,\text{Å}$, $E_F = 0.2\,\text{eV}$ [22], $J_{pd} = 0.15\,\text{eV-nm}^3$ [30], $S = 5/2$, $s = 1/2$, $g_h = g_{MN} = 2$, $p = 4.9 \times 10^{20}\,\text{cm}^{-3}$ [31] and $T_C = 110\,\text{K}$ for a sample with $x = 0.05$ [16]. The suitable parameter for the barrier height of GaAs is $\phi = 0.1\,\text{eV}$ [24].

It is important to note that in the valance band of semiconductors, there are heavy hole and light hole bands which are degenerate at the top of the valance band. Therefore, it seems to be reasonable that we use one value for the hole mass at the structures with low Mn concentration. Hence, the effective mass of all carriers are taken as $m^* = 0.16\,m_h$ (m_h is the free-hole mass), which is consistent with the experimental parameters used in the present work.

In Fig. 1 we have presented the TMR as a function of the applied voltage for several temperatures when $d = 0.565\,\text{nm}$. As it is evident from the figure, at all temperatures the TMR decreases monotonically as V_a increases. Also, it is seen that, the bias voltage values, where the TMR ratio reaches half its maximum, varies from 55 to 90 mV depending on temperature. This value is much smaller than that of metal-based single barrier MTJ structures (300–400 mV) [1,32,33]. At very low voltages, for both parallel and antiparallel alignments, the tunnel current densities vary linearly, therefore, the TMR behaves similar to a flat curve. However, with increasing the applied voltage, due to the modification of the barrier shape, a nearly parabolic dependence of currents on the voltage appears, and this modifies the TMR curve. With increasing the temperature, the spontaneous spin splitting in the

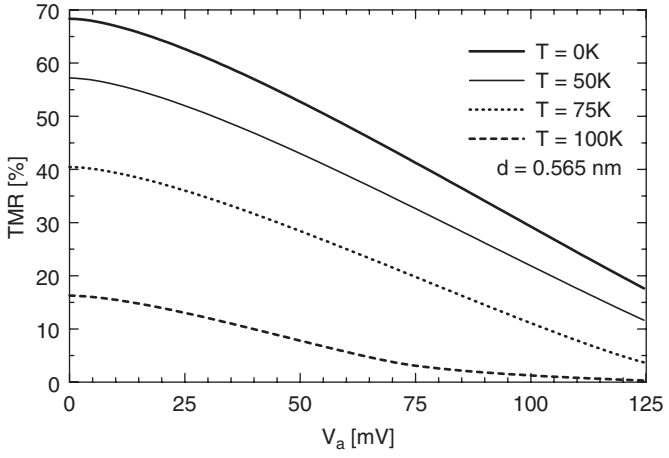

Fig. 1. Dependence of the TMR on the applied voltage at different temperatures.

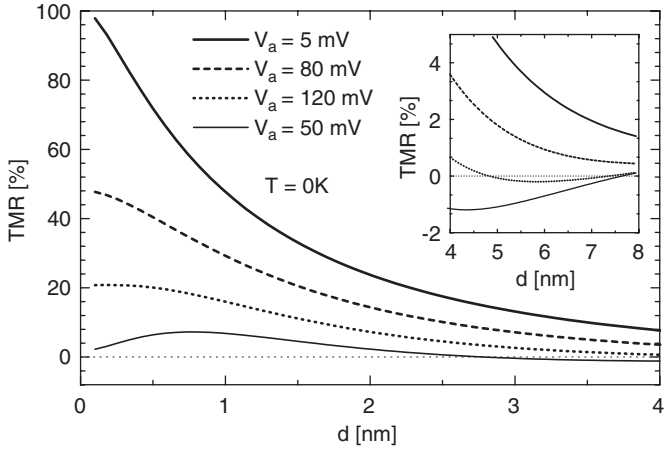

Fig. 2. Variations of the TMR as a function of the barrier thickness at different temperatures.

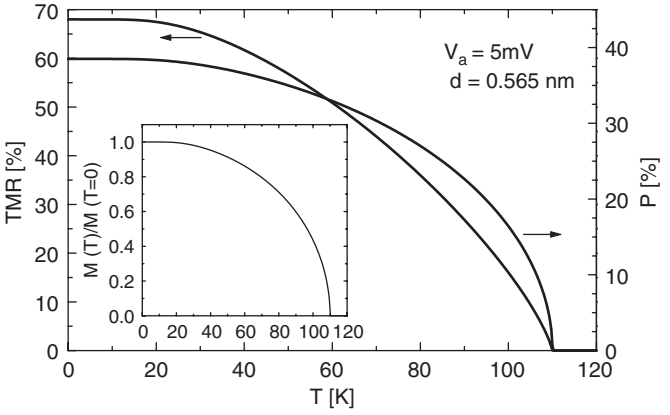

Fig. 3. Dependence of the TMR (left) and spin polarization (right) as a function of temperature. The inset shows temperature dependence of the normalized magnetization of $Ga_{0.95}Mn_{0.05}As$ electrodes.

valence band of the DMS layers decreases. In this case, the difference between current densities in both parallel and antiparallel configurations is also reduced. Thus, in such temperatures one can expect low values for TMR ratio, as it is clear in the figure. The results show that the discrepancy between the TMR (100 K) and TMR (0 K) decreases with increasing the bias voltage. Therefore, the applied bias has a strong influence on the TMR. The relative behavior of the curves in Fig. 1 is qualitatively in good agreement with the recent experimental results [24].

The barrier thickness dependence of TMR at different applied biases has been shown in Fig. 2. For $V_a = 5$ and 80 mV, with increasing the barrier thickness, the TMR decreases rapidly from its maximum value and always remains positive for various thicknesses of the GaAs layer. However, for $V_a = 120$ and 150 mV, it is found that the TMR becomes negative in a certain range of the barrier thickness, as it is shown in the inset. The origin of this effect is related to the enhancement of the applied bias and can be observed, when the applied bias is more than the barrier height (100 meV). In fact, at high voltage range ($eV_a > \phi$) a quantum well will appear at GaAs/GaMnAs interface; thus, the carriers at the Fermi level of the left electrode tunnel through the GaAs barrier and the quantum well into the right electrode. In this regard, the carriers can cause standing waves in the barrier, leading to a reduction and a sign reversal of the TMR, as it is shown in the inset of Fig. 2. Also, with further increasing of the applied voltage, the TMR exhibits a peak at low thicknesses, which has been observed previously in GaMnAs/AlAs/GaMnAs heterostructures [22].

The temperature dependence of the TMR and spin polarization is also calculated in the present MTJ. The results are shown in Fig. 3 at $V_a = 5$ mV when $d = 0.565$ nm. From the figure, it is clear that, both the TMR and spin polarization decrease with increasing temperature, and vanish at 110 K, which is the Curie temperature of the $Ga_{0.95}Mn_{0.05}As$ layers. One can see that the highest value of TMR (about 70%) and spin polarization (about 37%) can be obtained at zero temperature. The inset shows the normalized magnetization of $Ga_{0.95}Mn_{0.05}As$ layers as a function of temperature. The reduction of TMR and spin polarization arises as a result of the dependence of spin-splitting energy on temperature. The comparison of the present results and those obtained with experiment [24] shows somewhat different behavior at 10–30 K. Such discrepancy between our theory and the experiment can be probably due to the effects of magnetic anisotropy at the GaMnAs/GaAs interfaces and also spin-flip scattering at low temperature in the GaMnAs electrodes. The mean-field theory does not take into account the effects mentioned here.

Our final comment addresses the role of Rashba spin–orbit interaction in the present tunnel structure [34,35]. The Rashba effect produces a spin-flip scattering in the interfaces, which affect the transmission of each spin channel and cannot be solved separately. Therefore, a spin mixture occurs and the currents become less spin polarized. However, the Rashba effect is very small. In fact, with assuming the Rashba interaction in the MTJs, it has been shown that, the spin-dependent transmission coefficients change very small in both the parallel and antiparallel configurations [35]. Hence, the variation of spin polarization and TMR due to this effect is nearly small. Therefore, one can omit this effect in such tunnel heterostructure. That is, the Rashba effect does not have a dominant influence on the spin polarization and TMR.

4. Summary and conclusions

On the basis of the effective mass approximation model including the temperature dependence of spin splitting, we studied the spin-polarized tunneling in $Ga_{0.95}Mn_{0.05}As/GaAs/Ga_{0.95}Mn_{0.05}As$ heterostructure. The numerical results showed that the TMR strongly depends on GaAs barrier thickness, applied voltage and temperature. At high voltages, with increasing the barrier thickness, a peak and sign reversal was observed in the

TMR curves. Also, we found that, both the TMR and spin polarization decrease with increasing the temperature. The results obtained in this work show the main features of the experiments and can be a base for development for spin-dependent tunneling electronic devices.

References

[1] J.S. Moodera, L.R. Kinder, T.M. Wong, R. Meservey, Phys. Rev. Lett. 74 (1995) 3273.
[2] J. Daughton, J. Appl. Phys. 81 (1997) 3758.
[3] J.C. Slonczewski, Phys. Rev. B 39 (1989) 6995.
[4] E.Yu. Tsymbal, D.G. Pettifor, J. Phys.: condens. matter 9 (1997) L411.
[5] K. Wang, S. Zhang, P.M. Levy, L. Szunyogh, P. Weinberger, J. Magn. Magn. Mater. 189 (1998) L131.
[6] M. Tsunoda, K. Nishikawa, S. Ogata, M. Takahashi, Appl. Phys. Lett. 80 (2002) 3135.
[7] P. LeClair, J.K. Ha, H.J.M. Swagten, C.H. van de Vin, J.T. Kohlhepp, W.J.M. de Jonge, Appl. Phys. Lett. 80 (2002) 625.
[8] A. Saffarzadeh, J. Magn. Magn. Mater. 269 (2004) 327.
[9] A.A. Shokri, A. Saffarzadeh, J. Phys.: condens. matter 16 (2004) 4455.
[10] A.A. Shokri, A. Saffarzadeh, Eur. Phys. J. B 42 (2004) 187.
[11] D.C. Worledge, T.H. Geballe, J. Appl. Phys. 88 (2000) 5277.
[12] A.T. Filip, P. LeClair, C.J.P. Smits, J.T. Kohlhepp, H.J.M. Swagten, B. Koopmans, W.J.M. de Jonge, Appl. Phys. Lett. 81 (2002) 1815.
[13] A. Saffarzadeh, J. Phys.: condens. matter 15 (2003) 3041.
[14] M. Wilczyński, J. Barnaś, R. Świrkowicz, J. Magn. Magn. Mater. 267 (2003) 391.
[15] A. Mauger, C. Godart, Phys. Rep. 141 (1986) 51.
[16] H. Ohno, Science 281 (1998) 951;
H. Ohno, J. Magn. Magn. Mater. 200 (1999) 110.
[17] T. Dietl, H. Ohno, F. Matsukura, J. Cibert, D. Ferrand, Science 287 (2000) 1019.
[18] J. König, H.H. Lin, A.H. MacDonald, Phys. Rev. Lett. 84 (2000) 5628.
[19] T. Hayashi, M. Tanaka, A. Asamitsu, J. Appl. Phys. 87 (2000) 4673.
[20] T. Hayashi, M. Tanaka, K. Seto, T. Nishinaga, K. Ando, Appl. Phys. Lett. 71 (1997) 1825.
[21] D. Chiba, N. Akiba, F. Matsukura, Y. Ohno, H. Ohno, Appl. Phys. Lett. 77 (2000) 1873.
[22] M. Tanaka, Y. Higo, Phys. Rev. Lett. 87 (2001) 026602.
[23] Y. Ohno, I. Arata, F. Matsukura, H. Ohno, Physica E 13 (2002) 521.
[24] D. Chiba, F. Matsukara, H. Ohno, Physica E 21 (2004) 966.
[25] R. Mathieu, P. Savedlindh, J. Sadowski, K. Światek, M. Karlsteen, J. Kanski, L. IIver, Appl. Phys. Lett. 81 (2002) 3013.
[26] Y.C. Tao, J.G. Hu, H. Liu, J. Appl. Phys. 96 (2004) 498.
[27] M. Abramowitz, I.A. Stegun, Handbook of Mathematical Functions, Dover, New York, 1965.
[28] C.B. Duke, in: E. Burstein, S. Lundquist (Eds.), Tunneling Phenomena in Solids, Plenum, New York, 1969.
[29] S. Das Sarma, E.H. Hwang, A. Kaminski, Phys. Rev. B 67 (2003) 155201.
[30] T. Jungwirth, W.A. Atkinson, B.H. Lee, A.H. MacDonald, Phys. Rev. B 59 (1999) 9818.
[31] H. Ohno, F. Matsukura, T. Omiya, N. Akiba, J. Appl. Phys. 85 (1999) 4277.
[32] R.C. Sousa, J.J. Sun, V. Soares, P.P. Freitas, K. King, M.F. da Silva, J.C. Soares, Appl. Phys. Lett. 73 (1998) 3288.
[33] Y. Lu, X.W. Li, G. Xiao, R.A. Altman, W.J. Gallagher, A. Marley, K. Roche, S.S.P. Parkin, J. Appl. Phys. 83 (1998) 6515.
[34] S.S. Makler, M.A. Boselli, J. Weberszpil, X.F. Wang, I.C. da Cunha Lima, Physica B 320 (2002) 396.
[35] S.S. Makler, J.G. Zelcovit, M.A. Boselli, I.C. da Cunha Lima, Physica B 354 (2004) 348.